The protective effects of total paeony glycoside on ischemia/reperfusion injury in H9C2 cells via inhibition of the PI3K/Akt signaling pathway

PEIHONG SHEN[1*], JUNFENG CHEN[2*] and MIN PAN[1]

[1]Department of Integrated Traditional and Western Medicine, and General Family Medicine;
[2]Department of Respiration, The First People's Hospital of Wenling, Wenling, Zhejiang 317500, P.R. China

Received December 14, 2017; Accepted June 21, 2018

DOI: 10.3892/mmr.2018.9335

Abstract. At present, cardiovascular disease is the global leading cause of mortality. Total paeony glycoside (TPG) is a traditional Chinese medicine, which serves a pivotal role in the cardiovascular system. In the present study, the effects and underlying mechanisms of TPG on ischemia/reperfusion (I/R) injury-induced apoptosis of cardiomyocytes were investigated *in vitro*. Cell Counting kit-8 and flow cytometry were used to assess the viability, reactive oxygen species (ROS) content and apoptosis of H9C2 cells. The activities of lactate dehydrogenase (LDH), malondialdehyde (MDA), superoxide dismutase (SOD) and glutathione peroxidase (GPX) were analyzed by commercial detection kits. Reverse transcription-quantitative polymerase chain reaction and western blot analysis were conducted to evaluate the expression levels of various factors. The results demonstrated that the viability of H9C2 cells was not significantly altered in response to various concentrations of TPG. However, following I/R injury, TPG markedly enhanced cell viability in a time- and dose-dependent manner. Furthermore**,** TPG decreased the rate of apoptosis and ROS levels, and reduced the activities of MDA and LDH. Conversely, TPG increased SOD and GPX activities. In addition, TPG upregulated the expression levels of pro-caspase-3 and B-cell lymphoma2 (Bcl-2), whereas it downregulated cleaved-caspase-3, poly (ADP-ribose) polymerase 1, Bcl-2-associated X protein, phosphorylated (p)-phosphatidylinositol 3 kinase (PI3K) and p-protein kinase B (Akt) expression. Treatment with insulin-like growth factor-1 increased the apoptosis of H9C2 cells, thus suggesting that activation of the PI3K/Akt signaling pathway reversed the protective effects of TPG. Taken together, TPG may suppress I/R-induced apoptosis and oxidative stress of H9C2 cells possibly by inhibiting the PI3K/Akt signaling pathway; such a phenomenon may have a therapeutic effect on cardiovascular disease.

Correspondence to: Dr Min Pan, Department of Integrated Traditional and Western Medicine and General Family Medicine, The First People's Hospital of Wenling, 333 Chuanan Nan Road, Chengxi Street, Wenling, Zhejiang 317500, P.R. China
E-mail: minpan86pm@163.com

*Contributed equally

Key words: total paeony glycoside, cardiomyocytes, ischemia/reperfusion injury, apoptosis

Introduction

Cardiovascular disease is currently the global leading cause of mortality (1). It has previously been reported that acute myocardial infarction is a major cause of cardiovascular disease (2). When coronary artery occlusion occurs, in order to save the myocardial tissues, the infarct-associated artery is promptly opened and blood supply is restored to the ischemic myocardium. However, reperfusion causes damage to the cardiac structure, leading to the occurrence of cardiac arrest, decreased cardiac function and malignant cardiac arrhythmia. Such a phenomenon is known as ischemia/reperfusion (I/R) injury (3). I/R injury is a clinicopathological process in which varying levels of cardiomyocyte apoptosis can occur (4). I/R injury also induces oxidative stress (5,6); therefore, inhibition of apoptosis and oxidative stress may reduce damage.

Recently, studies have demonstrated that traditional Chinese medicine may be effective in the prevention and treatment of myocardial I/R injury (7,8). According to traditional Chinese medicine, Radix Paeoniae Rubra, the dried root of *Paeonia lactiflora* Pall, is able to reduce heat and cool blood, disperse stasis and relieve pain (9-11). Total paeony glycoside (TPG) is a major component of Radix Paeoniae Rubra, and the effective component of TPG is a monoterpene compound (12). Modern pharmacological studies have demonstrated that Radix Paeoniae Rubra has various pharmacological functions that mainly produce effects on the cardiovascular system (9,13,14). In addition, it exerts antitumor and anti-endotoxin effects, as well as other functions (9,13,14). Furthermore, TPG has been used to treat cancer, atherosclerosis and ischemic cerebrovascular disease in China (15,16). Previous studies have demonstrated that TPG is capable of preventing thrombosis, of inhibiting and scavenging oxygen free radicals, and of suppressing cell apoptosis (15,17,18); it also has the potential

to effectively protect liver and brain cells (15,19,20). However, whether it has such a protective effect on myocardial I/R injury remains unknown.

The phosphatidylinositol 3 kinase/protein kinase B (PI3K/Akt) signal transduction pathway is a critical pathway that serves a pivotal role in cell proliferation, apoptosis and differentiation (21,22). Furthermore, studies have demonstrated that the PI3K/Akt pathway is involved in I/R injury in various organs, including liver, brain and heart (23-25). However, whether the role of TPG in I/R injury is associated with this pathway remains unknown.

In the present study, the rat cardiac myoblast cell line H9C2 was selected to establish an I/R injury model *in vitro*. The effects and mechanism of TPG on the I/R-induced apoptosis and oxidative stress of H9C2 cells were subsequently investigated.

Materials and methods

Drug preparation. TPG powder was obtained from Haoxuan Biological Technology Co., Ltd. (Xi'an, China), which had been approved by the State Food and Drug Administration for clinical trials. The powder was dissolved in PBS, and the solution was filtered and sterilized using a 0.22-μm filter membrane (EMD Millipore, Billerica, MA, USA). Following filtration and sterilization, the solution was diluted to 10, 20, 40, 80, 160 and 320 μg/ml using PBS. Insulin-like growth factor (IGF)-1 was purchased from Sigma-Aldrich; Merck KGaA (Darmstadt, Germany); the final concentration used to activate PI3K/Akt was 100 ng/ml (26,27).

Cell culture. The H9C2 rat cardiac myoblast cell line was acquired from Cobioer Biosciences Co., Ltd. (Nanjing, China). Cells were maintained in complete high-glucose Dulbecco's Modified Eagle Medium (DMEM; Beijing Solarbio Science & Technology Co, Ltd., Beijing, China) supplemented with 10% fetal bovine serum (Hyclone; GE Healthcare Life Sciences, Logan, UT, USA) and 1% penicillin-streptomycin (Beijing Leagene Biotechnology Co., Ltd., Beijing, China) in an incubator containing 95% humidified air and 5% CO_2 at 37˚C.

Establishment of a myocardial I/R injury model. H9C2 cells were selected to establish an I/R model, according to a previous study (28). Briefly, cells were cultured at 37˚C for 48 h (95% humidified air and 5% CO_2). After cell culture, cells were incubated in serum- and glucose-free DMEM and were maintained in a low-oxygen incubator at 37˚C (95% N_2, 5% CO_2 and 1% O_2) for 10 h, in order to mimic hypoxia. Subsequently, cells were cultured in complete high-glucose DMEM and were maintained in an incubator containing 95% humidified air and 5% CO_2 at 37˚C for 2 h, in order to mimic re-oxygenation (reperfusion). Cells in the control group were cultured without any treatment at 37˚C (95% humidified air and 5% CO_2).

Cell Counting kit-8 (CCK-8) assay. Cell viability was evaluated using CCK-8 (Wuhan Merck Biotechnology Co., Ltd., Wuhan, China), according to the manufacturer's protocol. Briefly, cells were incubated in 96-well plates ($2.5x10^3$ cells/well) for 24 h at 37˚C. Subsequently, a portion of cells was treated with various concentrations of TPG (10, 20, 40, 80, 160 and 320 μg/ml) for 12, 24 and 48 h at 37˚C. Another portion of cells was used to establish the I/R injury model and were treated with low, medium or high concentrations of TPG (10, 40 and 160 μg/ml) for 12, 24 and 48 h at 37˚C. Subsequently, CCK-8 reagent was added to the cells, which were incubated for 4 h at 37˚C. The optical density (OD) value was measured at 450 nm using a light absorption microplate reader (ELx808; BioTek Instruments, Inc., Winooski, VT, USA). The concentrations of TPG used were adopted according to previous studies (18,29).

Reactive oxygen species (ROS) assay. ROS production was assessed using 2',7'-dichlorofluorescein diacetate (DCFH-DA; Sigma-Aldrich; Merck KGaA), according to the manufacturer's protocol. DCFH-DA can be oxidized by ROS into fluorescent DCF, and the fluorescent signal indicates ROS production. Briefly, cells were seeded at a density of $2.5x10^4$ cells/well into a 96-well plate, after which they were subjected to I/R injury and then treated with various concentrations of TPG (10, 40 and 160 μg/ml) for 24 h at 37˚C. Cells were subsequently incubated with 25 μM DCFH-DA at 37˚C for 30 min and were washed three times with PBS. ROS production was measured using a FACSCalibur flow cytometer with Cell Quest 3.3 software (BD Biosciences, Franklin Lakes, NJ, USA).

Cell apoptosis assay. The Annexin V-fluorescein isothiocyanate (FITC)/propidium iodide (PI) apoptosis detection kit (Shanghai Qcbio Science & Technologies Co., Ltd., Shanghai, China) was performed to determine cell apoptosis, according to the manufacturer's protocol. Briefly, cells were seeded at a density of $6x10^5$ cells/well in 6-well plates, after which they were subjected to I/R injury and then treated with 10 μg/ml TPG and 100 ng/ml IGF-1. Following cell treatment, the cells were rinsed three times with PBS. Subsequently, the cells were stained with Annexin V-FITC and PI solution in the dark at room temperature for 20 min. Finally, 1X Binding Buffer was added to the cells on ice and cell apoptosis was measured using flow cytometery.

Lactate dehydrogenase (LDH) assay. LDH activity was examined using a LDH detection kit (Shanghai Genmed Pharmaceutical Technology Co Ltd., Shanghai, China), according to the manufacturer's protocol. Following cell treatment, the cells were exposed to reagent A for 5 min at room temperature, and then to reagent B for 10 min at room temperature. Subsequently, cells were centrifuged at 300 x g for 5 min and the supernatant was added to 96-well plates, and fixed with reagent C and reagent D in the dark for 30 min at room temperature. Subsequently, reagent E was added to the mixture. The OD value was measured at 490 nm using a light absorption microplate reader.

Malondialdehyde (MDA) assay. The MDA detection kit (Beijing Leagene Biotechnology Co., Ltd.) was performed to detect MDA activity, according to the manufacturer's protocol. Following cell treatment, the cells were lysed on ice using an ATPIO-400SD ultrasonic cell breaker (Nanjing ATPIO Instruments Manufacture Co., Ltd., Nanjing, China). Subsequently, the cell lysate was mixed with TAB solution; the mixture was heated in boiling water for 10 min

Table I. Primer sequences.

Primer name	Sequence (5'-3')	Product size (bp)
Caspase-3-forward	TGGAATGTCAGCTCGCAATG	224
Caspase-3-reverse	CAGGTCCGTTCGTTCCAAAA	
Bax-forward	GAGACACCTGAGCTGACCTT	187
Bax-reverse	CGTCTGCAAACATGTCAGCT	
Bcl-2-forward	GCCTTCTTTGAGTTCGGTGG	221
Bcl-2-reverse	CTGAGCAGCGTCTTCAGAG	
PARP1-forward	CCAAGGCAGCAGTGAATCTC	205
PARP1-reverse	GGGGTCCTTACTGCTGTCAT	
β-actin-forward	TGTGTTGTCCCTGTATGCC	232
β-actin-reverse	AATGTCACGCACGATTTCCC	

Bax, Bcl-2-associated X protein; Bcl-2, B-cell lymphoma 2; PARP, poly (ADP-ribose) polymerase.

and centrifuged at 800 x g at room temperature for 5 min. Subsequently, the precipitate was resuspended in PBS. The OD value was measured at 532 nm using a light absorption microplate reader.

Superoxide dismutase (SOD) assay. SOD activity was identified using the SOD detection kit (Beyotime Institute of Biotechnology, Haimen, China), according to the manufacturer's protocol. Following cell treatment, the cells were lysed on ice using an ATPIO-400SD ultrasonic cell breaker. Subsequently, the cell lysate was mixed with hydroxylamine working fluid at 37˚C for 30 min. Subsequently, chromogenic reagent was added to the mixture for 16 min at room temperature. The OD value was measured at 550 nm using a light absorption microplate reader.

Glutathione peroxidase (GPX) assay. GPX activity was analyzed using a GPX detection kit (Beyotime Institute of Biotechnology), according to the manufacturer's protocol. Following cell treatment, the cells were lysed on ice using an ATPIO-400SD ultrasonic cell breaker. Subsequently, cells were mixed with peroxide solution at 25˚C for 10 min. The OD value at 430 nm was measured every 30 sec at 25˚C using a light absorption microplate reader.

Reverse transcription-quantitative polymerase chain reaction (RT-qPCR). Total RNA was extracted using the TRIzol® reagent (Invitrogen; Thermo Fisher Scientific, Inc., Waltham, MA, USA). RNA (1 μg) was used to synthesize cDNA by RevertAid™ cDNA Synthesis kit (Thermo Fisher Scientific, Inc.), according to the manufacturer's protocol. The PCR reaction mixture (50 μl) contained 25 μl Dream Taq Green PCR master Mix, 1 μl forward/reverse primer, 19 μl nuclease-free H_2O and 4 μl cDNA. Reaction conditions were as follows: Pre-denaturation at 96˚C for 4 min, followed by 30 cycles of denaturation at 96˚C for 20 sec and annealing at 60˚C for 30 sec, and final extension at 72˚C for 30 sec. The primers were purchased from Synbio Technologies, LLC (Suzhou, China) and are listed in Table I. β-actin was used as an internal control. The $2^{-\Delta\Delta Cq}$ method was used to compare the gene expression levels (30).

Western blot analysis. Cells were lysed with enhanced radioimmunoprecipitation assay buffer (Beijing Leagene Biotechnology Co., Ltd.) and total protein was extracted. The protein concentration was measured by bicinchoninic acid protein assay (Beyotime Institute of Biotechnology). A total of 25 μg protein was separated by 10% SDS-PAGE and bound to nitrocellulose membranes (Shanghai Kang Lang Biological Technology Co., Ltd., Shanghai, China). Membranes were blocked with 5% non-fat milk at 37˚C for 1 h. Subsequently, membranes were incubated with anti-pro-caspase-3 (cat. no. AF835, 1:1,000; R&D Systems, Inc., Minneapolis, MN, USA), anti-cleaved caspase-3 (cat. no. MAB835; 1:1,000; R&D Systems, Inc.), anti-cleaved poly (ADP-ribose) polymerase (PARP) 1 (cat. no. ab32561; 1:800; Abcam, Cambridge, UK), anti-B-cell lymphoma 2 (Bcl-2)-associated X protein (Bax; cat. no. MA5-14003; 1:1,000), anti-Bcl-2 (cat. no. MA5-11757; 1:1,000; both Invitrogen; Thermo Fisher Scientific, Inc.), anti-phosphorylated (p)-Akt (cat. no. AA329), anti-Akt (cat. no. AA326; 1:1,500; both Beyotime Institute of Biotechnology), anti-p-PI3K (cat. no. PA5-12799; 1:1,600), anti-PI3K (cat. no. MA5-17149; 1:1,000; both Invitrogen; Thermo Fisher Scientific, Inc.) and anti-β-actin (cat. no. MAB8969; 1:1,000; R&D Systems, Inc.) at 4˚C overnight. Subsequently, membranes were washed 2-4 times in TBS with 2% Tween-20 and were incubated with the following secondary antibodies: Mouse anti-rabbit immunoglobulin G (IgG) (cat. no. 3678; 1:8,000; Cell Signaling Technologies, Inc., Danvers, MA, USA), rabbit anti-mouse IgG (cat. no. 58802, 1:7,000; Cell Signaling Technologies, Inc.) and rabbit anti-goat IgG (cat. no. ab6741; 1:8,000; Abcam) for 1.5 h at room temperature. Proteins were detected using the iBright™ imaging system (A32749; Thermo Fisher Scientific, Inc.).

Statistical analysis. GraphPad Prism 6.0 (GraphPad Software, Inc., La Jolla, CA, USA) was used to perform the data analysis. The experimental data are presented as the means ± standard deviation. The differences between groups were assessed by one-way analysis of variance followed by Tukey's test. Each experiment was repeated at least three times. $P<0.05$ was considered to indicate a statistically significant difference.

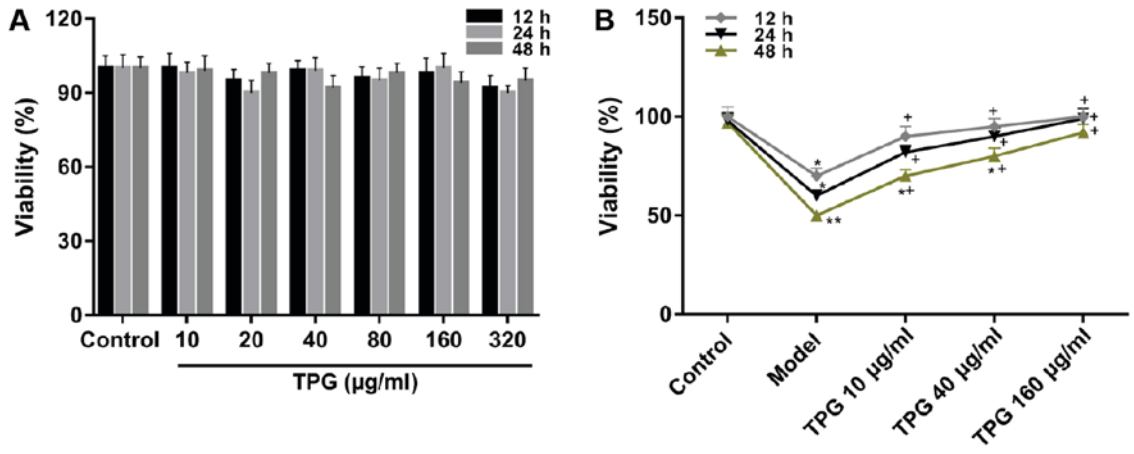

Figure 1. TPG elevates the viability of I/R-induced H9C2 cells. (A) Cell viability was examined using CCK-8. H9C2 cells were treated with TPG (10, 20, 40, 80, 160 and 320 μg/ml) for 12, 24 and 48 h. (B) H9C2 cells were impaired by I/R, and were treated with low, medium and high concentrations of TPG (10, 40 and 160 μg/ml, respectively) for 12, 24 and 48 h. *P<0.05, **P<0.01, vs. the control group; $^{+}$P<0.05, vs. the model group. I/R, ischemia/reperfusion; TPG, total paeony glycoside.

Results

TPG enhances the viability of H9C2 cells following I/R. CCK-8 was used to determine the effects of TPG on the viability of H9C2 cells. The CCK-8 assay results demonstrated that there was no alteration in viability when cells were treated with TPG alone (Fig. 1A). Additionally, when cells were impaired by I/R, cell viability was attenuated compared with in the control group. Conversely, TPG could significantly enhance the viability of cells inhibited by I/R in a time- and concentration-dependent manner compared with in the model group (P<0.05; Fig. 1B).

TPG inhibits I/R-induced apoptosis of H9C2 cells. To investigate the effects of TPG on the apoptosis of H9C2 cells, the Annexin V-FITC/PI apoptosis detection kit, RT-qPCR and western blotting were performed to measure the rates of apoptosis, and the mRNA and the protein expression levels of apoptosis-associated factors, respectively. The results of flow cytometry revealed that the rates of apoptosis were 4.93 and 19.00% in the control and model groups, respectively. In the 10, 40 and 160 μg/ml TPG groups the rates of apoptosis were 9.88, 6.94 and 5.27%, respectively. Compared with in the model group, apoptosis was reduced by TPG (P<0.05; Fig. 2). In addition, TPG markedly promoted the expression levels of pro-caspase-3 and Bcl-2, and suppressed the expression levels of cleaved-caspase-3, cleaved-PARP1 and Bax in a concentration-dependent manner, compared within the model group (P<0.05; Fig. 3).

TPG suppresses I/R-induced oxidative stress in H9C2 cells. To analyze whether TPG affects the oxidative stress of H9C2 cells, ROS levels and the activities of LDH, MDA, SOD and GPX were determined using various kits. The ROS assay results demonstrated that the ROS levels according to mean fluorescence intensity were 59.69, 195.34, 142.44, 109.22, and 75.95 in the control, model and TPG (10, 40 and 160 μg/ml) groups, respectively. ROS levels were increased in the model group compared with in the control group. Conversely, the ROS levels were decreased by 52.9, 86.12 and 119.39% in the TPG (10, 40 and 160 μg/ml) groups compared with in the model group (P<0.05; Fig. 4). Furthermore, TPG markedly reduced the activities of LDH and MDA; however, it promoted SOD and GPX activities in a concentration-dependent manner compared with in the model group (P<0.05; Fig. 5).

TPG suppresses the PI3K/Akt signaling pathway in H9C2 cells following I/R. In order to further investigate the molecular mechanism underlying the inhibitory effects of TPG on I/R-induced apoptosis of H9C2 cells, the protein expression levels of p-PI3K, PI3K, p-Akt and Akt were detected by western blot analysis. The results revealed that compared with in the model group, the expression levels of p-PI3K and p-Akt were attenuated in response to TPG (10, 40 and 160 μg/ml; P<0.05). However, no changes were detected in total PI3K and Akt protein expression among the various groups (Fig. 6).

IGF-1 reverses the effects of TPG on I/R injury. As previously described, IGF-1 is able to activate the PI3K/Akt signaling pathway (31). In the present study, IGF-1 was used to investigate the association of the PI3K/Akt signaling pathway with the protective effects of TPG against I/R injury. I/R-induced apoptosis was attenuated by TPG. Conversely, the number of apoptotic cells in the TPG + IGF-1 group was increased compared with in the TPG group, thus suggesting that IGF-1 treatment reversed the effects of TPG (Fig. 7).

Discussion

Traditional Chinese medicine has been widely used to treat various diseases in medical practice. TPG is a traditional Chinese medicine, which possesses antitumor effects and is able to target cardiovascular and cerebrovascular diseases (15,16). Furthermore, previous studies have reported that TPG regulates cell proliferation and apoptosis (17,18). Therefore, in the present study, the effects of TPG on the viability and apoptosis of I/R-induced H9C2 cells were examined. The present results demonstrated that TPG alone did not affect H9C2 cell viability. However, TPG significantly promoted the

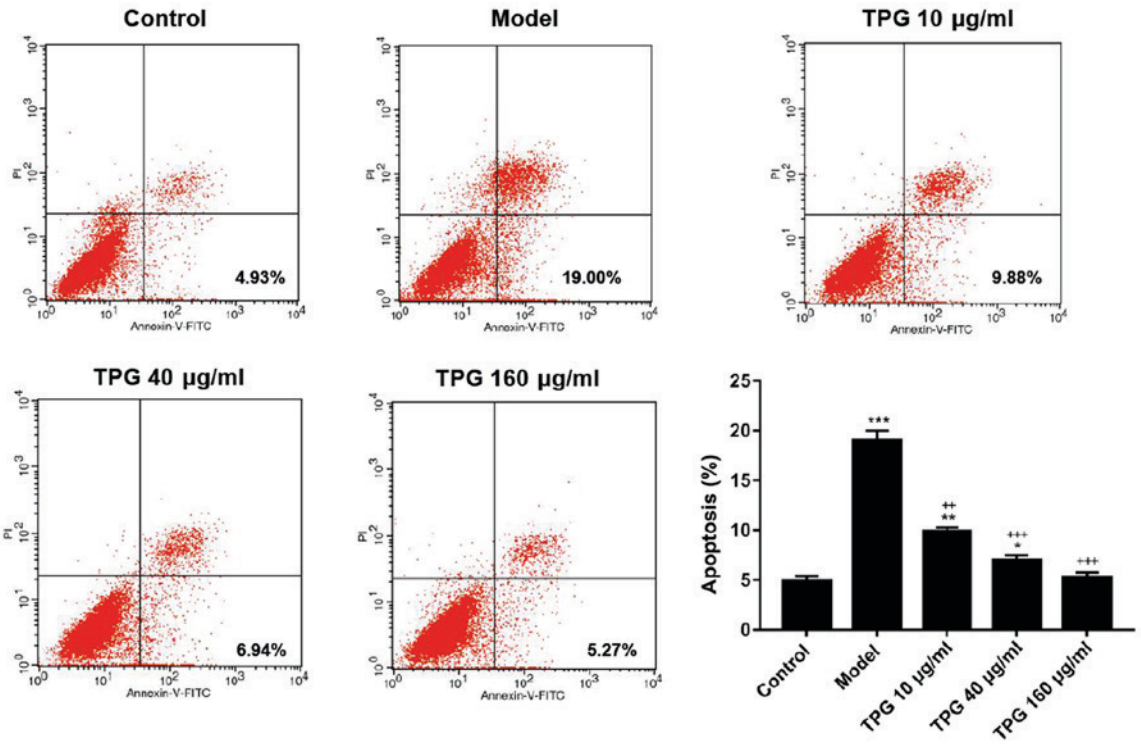

Figure 2. TPG inhibits the apoptosis of H9C2 cells induced by I/R. H9C2 cells were subjected to I/R injury and then treated with TPG (10, 40 and 160 μg/ml). The rate of apoptosis was assessed using the Annexin V-FITC/PI apoptosis detection kit. *P<0.05, **P<0.01, ***P<0.001, vs. the control group; $^{++}$P<0.01, $^{+++}$P<0.001, vs. the model group. FITC, fluorescein isothiocyanate; I/R, ischemia/reperfusion; PI, propidium iodide; TPG, total paeony glycoside.

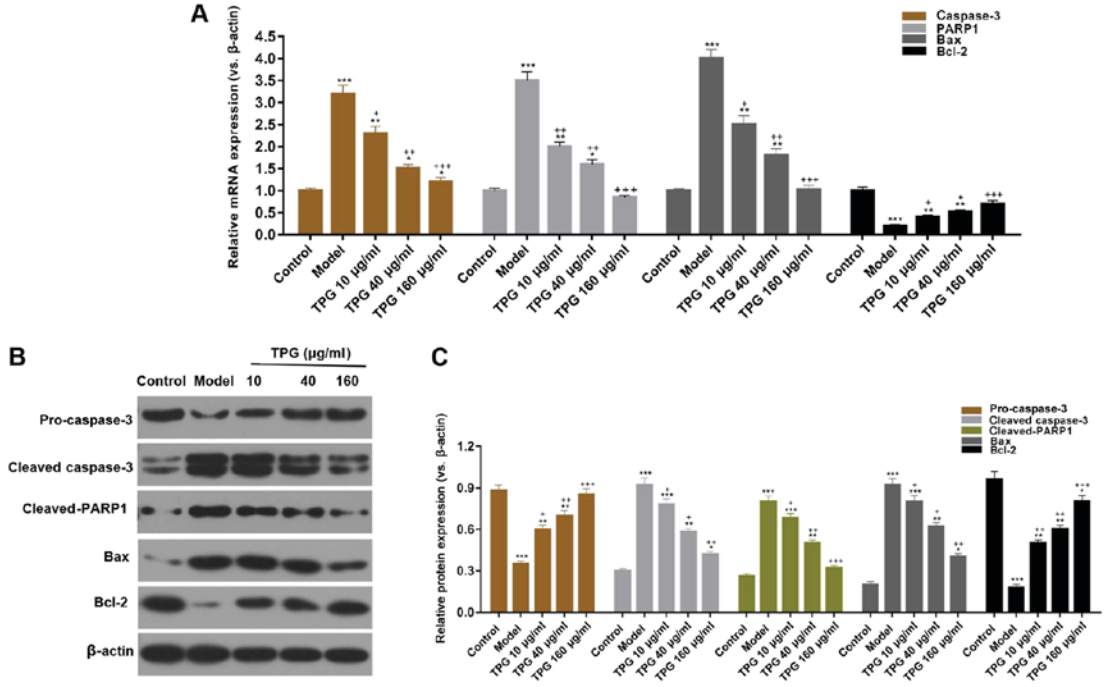

Figure 3. TPG regulates apoptosis-associated factors in H9C2 cells. H9C2 cells were treated with TPG (10, 40 and 160 μg/ml) for 24 h and subjected to I/R injury. (A) Relative mRNA expression levels of caspase-3, PARP1, Bax and Bcl-2 were investigated by reverse transcription-quantitative polymerase chain reaction. (B) Relative protein expression levels of caspase-3, PARP1, Bax and Bcl-2 were evaluated by western blotting and normalized to β-actin expression. (C) Blot results were semi-quantified. *P<0.05, **P<0.01, ***P<0.001, vs. the control group; $^{+}$P<0.05, $^{++}$P<0.01, $^{+++}$P<0.001, vs. the model group. Bax, Bcl-2-associated X protein; Bcl-2, B-cell lymphoma; I/R, ischemia/reperfusion; PARP, poly (ADP-ribose) polymerase; TPG, total paeony glycoside.

viability of H9C2 cells following I/R, and restrained apoptosis in a dose-dependent manner, thus suggesting that TPG exerts protective effects on an I/R injury model *in vitro*.

It has been reported that myocardial I/R is closely associated with myocardial cell apoptosis (32,33). Among the apoptosis-associated genes, Bcl-2 is an inhibitor of apoptosis

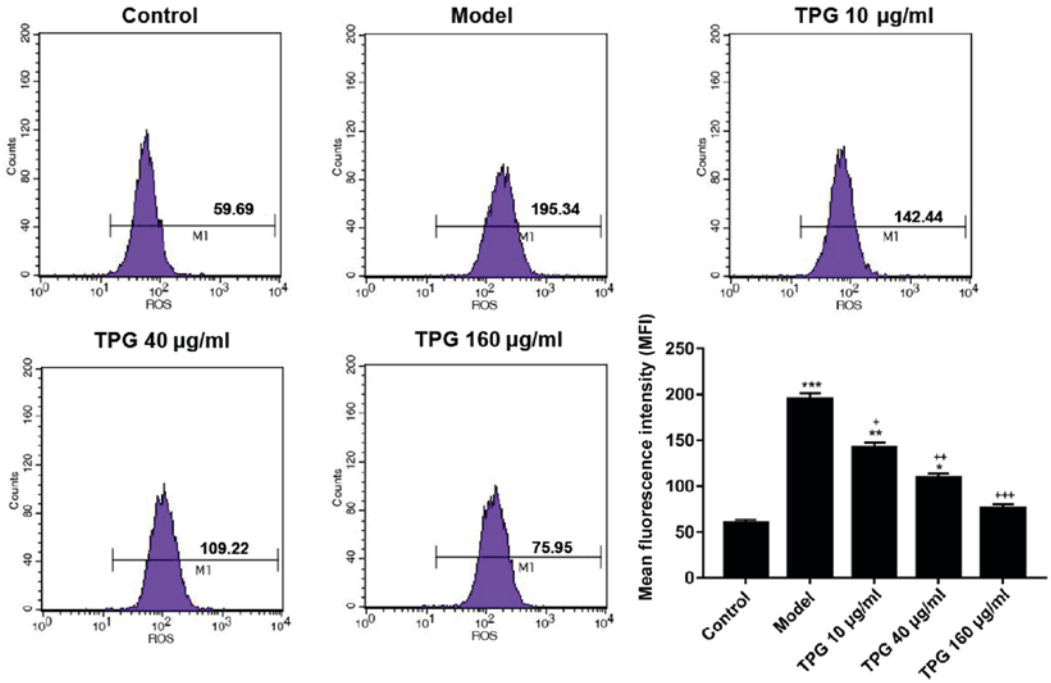

Figure 4. TPG inhibits I/R-induced ROS production in H9C2 cells. H9C2 cells were treated with TPG (10, 40 and 160 μg/ml) for 24 h and subjected to I/R injury. ROS production was detected using a ROS detection kit. *P<0.05, **P<0.01, ***P<0.001, vs. the control group; $^{+}$P<0.05, $^{++}$P<0.01, $^{+++}$P<0.001, vs. the model group. I/R, ischemia/reperfusion; ROS, reactive oxygen species; TPG, total paeony glycoside.

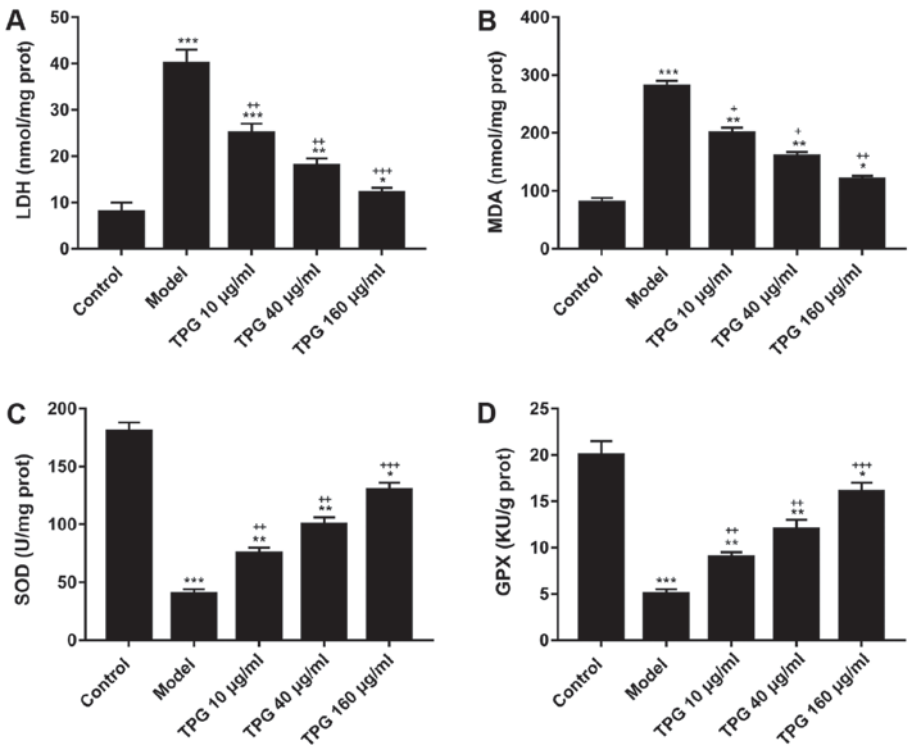

Figure 5. TPG suppresses LDH and MDA activities, and enhances SOD and GPX activities in I/R-induced H9C2 cells. H9C2 cells were treated with TPG (10, 40 and 160 μg/ml) for 24 h and subjected to I/R injury. (A) LDH activity, (B) MDA activity, (C) SOD activity and (D) GPX activity were detected. *P<0.05, **P<0.01, ***P<0.001, vs. the control group; $^{+}$P<0.05, $^{++}$P<0.01, $^{+++}$P<0.001, vs. the model group. GPX, glutathione peroxidase; I/R, ischemia/reperfusion; LDH, lactate dehydrogenase; MDA, malondialdehyde; SOD, superoxide dismutase; TPG, total paeony glycoside.

and Bax is a pro-apoptotic gene; the interaction between these two proteins regulates apoptosis (34,35). Furthermore, Bcl-2 can inhibit the activity of caspase-3, thus suppressing cell apoptosis (35). In addition, PARP1 is the most important substrate of caspase-3, which is involved in DNA repair and gene integrity monitoring; cleaved-PARP1 is a marker of apoptosis (36,37). Therefore, the role of TPG in inhibiting apoptosis induced by I/R was investigated by detecting

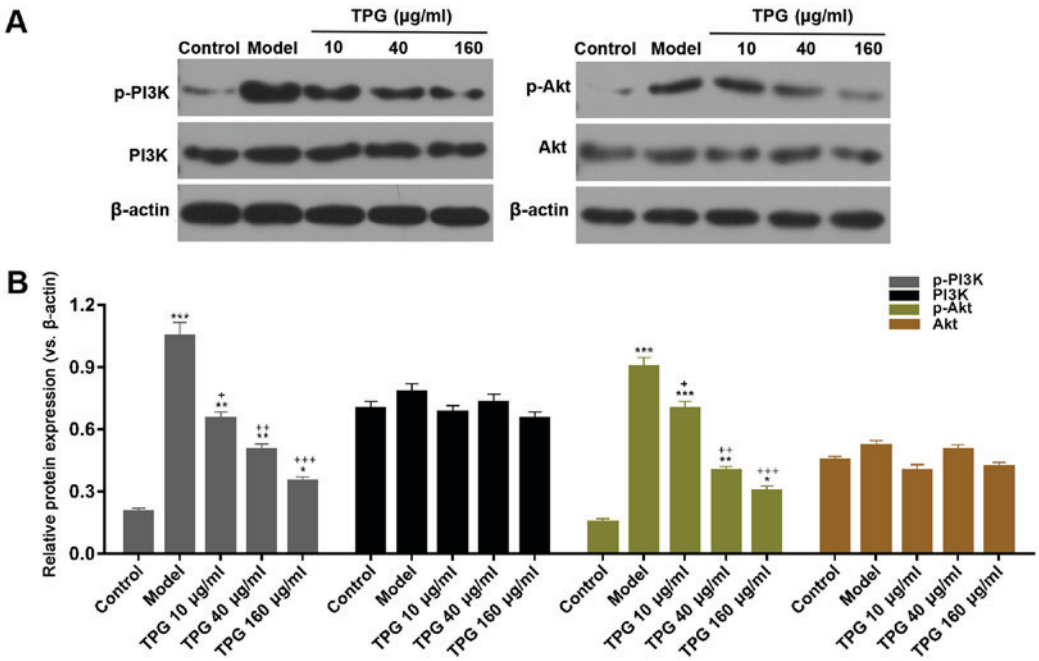

Figure 6. TPG suppresses the PI3K/Akt signaling pathway in I/R-induced H9C2 cells. H9C2 cells were treated with TPG (10, 40 and 160 μg/ml) for 24 h and subjected to I/R injury. (A) Relative protein expression levels of p-PI3K, PI3K, p-Akt and Akt were assessed by western blotting. β-actin was used as an internal control. (B) Blot results were semi-quantified. *P<0.05, **P<0.01, ***P<0.001, vs. the control group; $^{+}$P<0.05, $^{++}$P<0.01, $^{+++}$P<0.001, vs. the model group. Akt, protein kinase B; I/R, ischemia/reperfusion; p, phosphorylated; PI3K, phosphatidylinositol 3 kinase; TPG, total paeony glycoside.

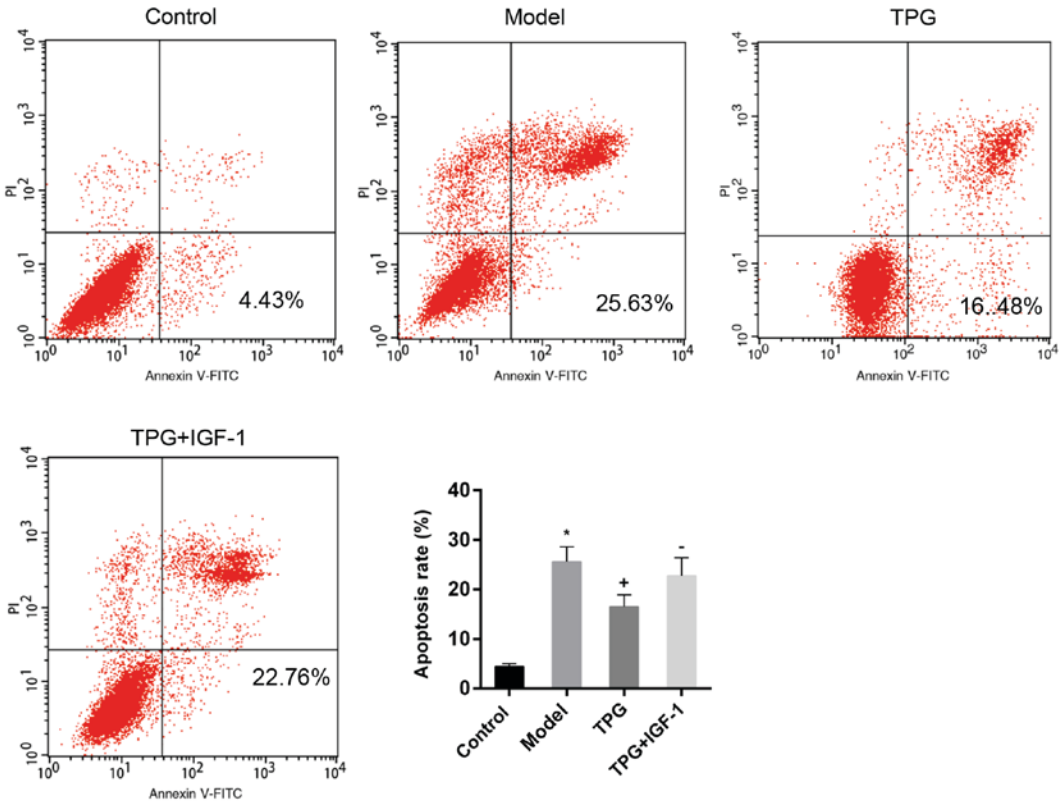

Figure 7. Treatment with IGF-1 enhances I/R-induced apoptosis of H9C2 cells. H9C2 cells were treated with 10 μg/ml TPG for 24 h prior to I/R injury. In the TPG + IGF-1 group, the cells were treated with 100 ng/ml IGF-1 to activate PI3K/Akt signaling. Cell apoptosis was measured by flow cytometry. *P<0.05 vs. the control group; $^{+}$P<0.05 vs. the model group, $^{-}$P<0.05 vs. the TPG group. Akt, protein kinase B; FITC, fluorescein isothiocyanate; IGF, insulin-like growth factor; I/R, ischemia/reperfusion; PI, propidium iodide; PI3K, phosphatidylinositol 3 kinase; TPG, total paeony glycoside.

the expression levels of these apoptosis-associated factors. The results demonstrated that TPG markedly upregulated the expression levels of pro-caspase-3 and Bcl-2, whereas it downregulated cleaved-caspase-3, cleaved-PARP1 and Bax

expression. Therefore, it was suggested that TPG inhibited I/R injury-induced apoptosis *in vitro*.

Oxidative stress is another important factor in the process of myocardial injury, which is characterized by the accumulation of ROS, increased nicotinamide adenine dinucleotide phosphate-oxidase and decreased antioxidant enzymes (38,39). A previous study demonstrated that sodium thiosulfate conspicuously reduces I/R damage-induced oxidative stress in rat hearts, and decreases the ROS levels, and LDH and MDA activities; however, it enhances SOD and GPX activities (40). Similar to previous studies, the present data revealed that TPG markedly reduced ROS levels, and LDH and MDA activities, whereas it increased the activities of SOD and GPX. Therefore, the present results indicated that TPG may reduce I/R-induced oxidative stress.

Previous studies have suggested that the PI3K/Akt signaling pathway is involved in the apoptosis of various tumor cells (41,42). Furthermore, it has been revealed that certain drugs could decrease apoptosis and oxidative stress of cells via regulation of the PI3K/Akt signaling pathway (41,43,44). Numerous drugs and proteins exert potential protective effects on myocardial injury via regulation of the PI3K/Akt signaling pathway (45-47). As expected, the present study observed that TPG significantly downregulated the phosphorylation levels of PI3K and Akt. Furthermore, apoptosis was increased by IGF-1, thus suggesting that the effects of TPG may be reversed by the activation of PI3K/Akt. Therefore, it may be suggested that TPG inhibited apoptosis and oxidative stress induced by myocardial I/R injury via restraining PI3K/Akt signaling; however, this requires further validation.

In conclusion, TPG facilitated cell viability, and suppressed I/R-induced apoptosis and oxidative stress in H9C2 cells, possibly via inhibiting the PI3K/Akt signaling pathway. Therefore, TPG may be of clinical significance in the treatment of cardiovascular diseases; however, this requires further investigation.

Acknowledgements

Not applicable.

Funding

No funding was received.

Availability of data and materials

All data generated or analyzed during this study are included in this published article.

Authors' contributions

PS and MP conceived and designed the study. JC analyzed and interpreted the data. PS drafted the manuscript. All authors were responsible for approving the final version of the manuscript.

Ethics approval and consent to participate

Not applicable.

Patient consent for publication

Not applicable.

Competing interests

The authors declare that they have no competing interests.

References

1. Kim Y, Keogh JB and Clifton PM: Benefits of nut consumption on insulin resistance and cardiovascular risk factors: Multiple potential mechanisms of actions. Nutrients 9: pii: E1271, 2017.
2. McCarthy CP, Bhambhani V, Pomerantsev E and Wasfy JH: In-hospital outcomes in invasively managed acute myocardial infarction patients who receive morphine. J Interv Cardiol 31: 150-158, 2018.
3. Jennings RB, Sommers HM, Smyth GA, Flack HA and Linn H: Myocardial necrosis induced by temporary occlusion of a coronary artery in the dog. Arch Pathol 70: 68-78, 1960.
4. Sodha NR, Clements RT, Feng J, Liu Y, Bianchi C, Horvath EM, Szabo C and Sellke FW: The effects of therapeutic sulfide on myocardial apoptosis in response to ischemia-reperfusion injury. Eur J Cardiothorac Surg 33: 906-913, 2008.
5. Gorenkova N, Robinson E, Grieve DJ and Galkin A: Conformational change of mitochondrial complex I increases ROS sensitivity during ischemia. Antioxid Redox Signal 19: 1459-1468, 2013.
6. Ekeløf S, Jensen SE, Rosenberg J and Gögenur I: Reduced oxidative stress in STEMI patients treated by primary percutaneous coronary intervention and with antioxidant therapy: A systematic review. Cardiovasc Drugs Ther 28: 173-181, 2014.
7. Han J, Wang D, Ye L, Li P, Hao W, Chen X, Ma J, Wang B, Shang J, Li D and Zheng Q: Rosmarinic acid protects against inflammation and cardiomyocyte apoptosis during myocardial ischemia/reperfusion injury by activating peroxisome proliferator-activated receptor gamma. Front Pharmacol 8: 456, 2017.
8. Zhang X, Du Q, Yang Y, Wang J, Dou S, Liu C and Duan J: The protective effect of Luteolin on myocardial ischemia/reperfusion (I/R) injury through TLR4/NF-κB/NLRP3 inflammasome pathway. Biomed Pharmacother 91: 1042-1052, 2017.
9. Chang CC, Yuan W, Lin YL, Liu RS, Juan YC, Sun WH, Tsay HJ, Huang HC, Lee YC and Liu HK: Evaluation of the in vivo therapeutic effects of radix paeoniae rubra ethanol extract with the hypoglycemic activities measured from multiple cell-based assays. Evid Based Complement Alternat Med 2016: 3262790, 2016.
10. Huang YQ, Ma X, Wang J, Zhao YL, Wang JB, Chen Z, Zhu Y, Shan LM, Wei SZ, Wang J and Xiao XH: Therapeutic efficacy and safety of paeoniae radix rubra formulae in relieving hyperbilirubinemia induced by viral hepatitis: A meta-analysis. Front Pharmacol 7: 63, 2016.
11. Xie P, Cui L, Shan Y and Kang WY: Antithrombotic effect and mechanism of radix paeoniae rubra. Biomed Res Int 2017: 9475074, 2017.
12. Dou ZH, Luo L and Lu D: Purification of total paeony glycoside by macroporous resin with double indices of albiflorin and paeoniflorin. Zhong Yao Cai 32: 1282-1284, 2009 (In Chinese).
13. Lin MY, Chiang SY, Li YZ, Chen MF, Chen YS, Wu JY and Liu YW: Anti-tumor effect of Radix Paeoniae Rubra extract on mice bladder tumors using intravesical therapy. Oncol Lett 12: 904-910, 2016.
14. Zhan LY, Xia ZY, Chen C and Wang XY: Effect of Radix Paeoniae Rubra on the expression of HO-1 and iNOS in rats with endotoxin-induced acute lung injury. Chin J Traumatol 9: 181-186, 2006.
15. Gu JF, Feng L, Yuan JR, Zhang MH and Jia XB: Effect of different composition structures of total paeony glycoside component and total phenolic acid component of Chuanxiong Rhizome on human umbilical vein endothelial cells with hypoxic injury. Zhongguo Zhong Yao Za Zhi 40: 920-926, 2015 (In Chinese).
16. Xu HY, Chen ZW and Wu YM: Antitumor activity of total paeony glycoside against human chronic myelocytic leukemia K562 cell lines in vitro and in vivo. Med Oncol 29: 1137-1147, 2012.

17. Liu C, Wang J and Yang J: Study on activating blood and eliminating stasis of total paeony glycoside(TPG). Zhong Yao Cai 23: 557-560, 2000 (In Chinese).
18. Long J, Gao M, Kong Y, Shen X, Du X, Son YO, Shi X, Liu J and Mo X: Cardioprotective effect of total paeony glycosides against isoprenaline-induced myocardial ischemia in rats. Phytomedicine 19: 672-676, 2012.
19. Ma RQ, Chen JW, Pang JX, Lan XJ and Qiu CH: Protective effects of total paeony glycoside against global cerebral ischemia-reperfusion injury in gerbils. Di Yi Jun Yi Da Xue Xue Bao 25: 471-473, 2005 (In Chinese).
20. Yang J, Wang J and Liu C: Protective effects of total paeony glycoside on cerebral ischemia mice. Zhong Yao Cai 24: 124-126, 2001 (In Chinese).
21. Parcellier A, Tintignac LA, Zhuravleva E and Hemmings BA: PKB and the mitochondria: AKTing on apoptosis. Cell Signal 20: 21-30, 2008.
22. Pei R, Si T, Lu Y, Zhou JX and Jiang L: Salvianolic acid A, a novel PI3K/Akt inhibitor, induces cell apoptosis and suppresses tumor growth in acute myeloid leukemia. Leuk Lymphoma 59: 1959-1967, 2018.
23. Zhang R, Zhang L, Manaenko A, Ye Z, Liu W and Sun X: Helium preconditioning protects mouse liver against ischemia and reperfusion injury through the PI3K/Akt pathway. J Hepatol 61: 1048-1055, 2014.
24. Zhao X, Xiang Y, Cai C, Zhou A, Zhu N and Zeng C: Schisandrin B protects against myocardial ischemia/reperfusion injury via the PI3K/Akt pathway in rats. Mol Med Rep 17: 556-561, 2018.
25. Zhou J, Du T, Li B, Rong Y, Verkhratsky A and Peng L: Crosstalk between MAPK/ERK and PI3K/AKT signal pathways during brain ischemia/reperfusion. ASN Neuro 7: pii: 1759091415602463, 2015.
26. Macrae VE, Ahmed SF, Mushtaq T and Farquharson C: IGF-I signalling in bone growth: Inhibitory actions of dexamethasone and IL-1beta. Growth Horm IGF Res 17: 435-439, 2007.
27. Wang H, Zhang Q, Zhang L, Little PJ, Xie X, Meng Q, Ren Y, Zhou L, Gao G, Quirion R and Zheng W: Insulin-like growth factor-1 induces the phosphorylation of PRAS40 via the PI3K/Akt signaling pathway in PC12 cells. Neurosci Lett 516: 105-109, 2012.
28. Wu WY, Wang WY, Ma YL, Yan H, Wang XB, Qin YL, Su M, Chen T and Wang YP: Sodium tanshinone IIA silate inhibits oxygen-glucose deprivation/recovery-induced cardiomyocyte apoptosis via suppression f the NF-κB/TNF-α pathway. Br J Pharmacol 169: 1058-1071, 2013.
29. He LN, Yang J, He SB, Wang J and Liu C: Protective effect of total paeony glocoside against ischemia injury in cultured primary cortex neurons. Chin J Clin Pharmacol Therapeut 1:1–6, 2000.
30. Livak KJ and Schmittgen TD: Analysis of relative gene expression data using real-time quantitative PCR and the 2(-Delta Delta C(T)) method. Methods 25: 402-408, 2001.
31. Stitt TN, Drujan D, Clarke BA, Panaro F, Timofeyva Y, Kline WO, Gonzalez M, Yancopoulos GD and Glass DJ: The IGF-1/PI3K/Akt pathway prevents expression of muscle atrophy-induced ubiquitin ligases by inhibiting FOXO transcription factors. Mol Cell 14: 395-403, 2004.
32. Chua CC, Gao J, Ho YS, Xiong Y, Xu X, Chen Z, Hamdy RC and Chua BH: Overexpression of IAP-2 attenuates apoptosis and protects against myocardial ischemia/reperfusion injury in transgenic mice. Biochim Biophys Acta 1773: 577-583, 2007.
33. Yaomura T, Tsuboi N, Urahama Y, Hobo A, Sugimoto K, Miyoshi J, Matsuguchi T, Reiji K, Matsuo S and Yuzawa Y: Serine/threonine kinase, Cot/Tpl2, regulates renal cell apoptosis in ischaemia/reperfusion injury. Nephrology (Carlton) 13: 397-404, 2008.
34. Raza A, Dikdan G, Desai KK, Shareef A, Fernandes H, Aris V, de la Torre AN, Wilson D, Fisher A, Soteropoulos P and Koneru B: Global gene expression profiles of ischemic preconditioning in deceased donor liver transplantation. Liver Transpl 16: 588-599, 2010.
35. Tsujimoto Y, Finger LR, Yunis J, Nowell PC and Croce CM: Cloning of the chromosome breakpoint of neoplastic B cells with the t(14;18) chromosome translocation. Science 226: 1097-1099, 1984.
36. Wesierska-Gadek J, Gueorguieva M, Wojciechowski J and Tudzarova-Trajkovska S: In vivo activated caspase-3 cleaves PARP-1 in rat liver after administration of the hepatocarcinogen N-nitrosomorpholine (NNM) generating the 85 kDa fragment. J Cell Biochem 93: 774-787, 2004.
37. Woo M, Hakem R, Soengas MS, Duncan GS, Shahinian A, Kägi D, Hakem A, McCurrach M, Khoo W, Kaufman SA, *et al*: Essential contribution of caspase 3/CPP32 to apoptosis and its associated nuclear changes. Genes Dev 12: 806-819, 1998.
38. Ansley DM and Wang B: Oxidative stress and myocardial injury in the diabetic heart. J Pathol 229: 232-241, 2013.
39. Elahi MM, Flatman S and Matata BM: Tracing the origins of postoperative atrial fibrillation: The concept of oxidative stress-mediated myocardial injury phenomenon. Eur J Cardiovasc Prev Rehabil 15: 735-741, 2008.
40. Ravindran S, Boovarahan SR, Shanmugam K, Vedarathinam RC and Kurian GA: Sodium thiosulfate preconditioning ameliorates ischemia/reperfusion injury in rat hearts via reduction of oxidative stress and apoptosis. Cardiovasc Drugs Ther 31: 511-524, 2017.
41. Ni Z and Yi J: Oxymatrine induces nasopharyngeal cancer cell death through inhibition of PI3K/AKT and NFκB pathways. Mol Med Rep 16: 9701-9706, 2017.
42. Xu H, Zou S and Xu X: The β-glucan from Lentinus edodes suppresses cell proliferation and promotes apoptosis in estrogen receptor positive breast cancers. Oncotarget 8: 86693-86709, 2017.
43. Hui Y, Chengyong T, Cheng L, Haixia H, Yuanda Z and Weihua Y: Resveratrol attenuates the cytotoxicity induced by amyloid-β1-42 in PC12 cells by upregulating heme oxygenase-1 via the PI3K/Akt/Nrf2 pathway. Neurochem Res 43: 297-305, 2018.
44. Li Y, Xia J, Jiang N, Xian Y, Ju H, Wei Y and Zhang X: Corin protects H_2O_2-induced apoptosis through PI3K/AKT and NF-κB pathway in cardiomyocytes. Biomed Pharmacother 97: 594-599, 2018.
45. Ha T, Hua F, Liu X, Ma J, McMullen JR, Shioi T, Izumo S, Kelley J, Gao X, Browder W, *et al*: Lipopolysaccharide-induced myocardial protection against ischaemia/reperfusion injury is mediated through a PI3K/Akt-dependent mechanism. Cardiovasc Res 78: 546-553, 2008.
46. Tang L, Mo Y, Li Y, Zhong Y, He S, Zhang Y, Tang Y, Fu S, Wang X and Chen A: Urolithin A alleviates myocardial ischemia/reperfusion injury via PI3K/Akt pathway. Biochem Biophys Res Commun 486: 774-780, 2017.
47. Thokala S, Inapurapu S, Bodiga VL, Vemuri PK and Bodiga S: Loss of ErbB2-PI3K/Akt signaling prevents zinc pyrithione-induced cardioprotection during ischemia/reperfusion. Biomed Pharmacother 88: 309-324, 2017.